Semi-Blind ML Synchronization for UWB Systems*

Stefan Franz[†], Cecilia Carbonelli[‡], Urbashi Mitra[†]

[†]Communication Sciences Institute, University of Southern California
3740 McClintock Avenue, Los Angeles, CA, 90089,
{sfranz,ubli}@usc.edu

[‡]Department of Information Engineering, University of Pisa
Via Caruso 2, 56100 Pisa, Italy,
cecilia.carbonelli@iet.unipi.it

Abstract

Synchronization is one of the most critical issues in PPM/TH ultra-wideband (UWB) communications due to the short duration of the pulses. In this work, we study a semi-blind synchronization scheme based on maximum-likelihood (ML) techniques to recover both symbol and frame timing. The proposed algorithm offers rapid acquisition and is robust against small timing errors due to a joint timing and channel estimate. The performance of the proposed algorithm is analyzed based on correlated Gaussian random variables and shown to be accurate for moderate to high SNR values.

1 Introduction

In ultra-wideband communications (UWB), communications information is conveyed with a train of ultra short and very low power spectral density pulses [10]. A key advantage of UWB signalling is its robustness against multipath fading. To fully exploit this feature, optimized matched filter detection requires knowledge of the channel response (CR). However, due to the large delay spread and large bandwidth inherent in UWB systems, channel estimation can be particularly cumbersome. An alternative to RAKE-type receivers are transmitted reference (TR) systems which do not require explicit channel estimation but rely on the transmission of unmodulated reference frames to form a template that is correlated with the incoming waveform [6]. Both, TR receivers, as well as coherent detectors need to know the timing of each symbol before performing data detection. Due to the short duration of the pulses, timing acquisition is a challenging task in the context of UWB communications and timing errors as small as fractions of nanoseconds can seriously degrade the system performance [9].

In UWB communications, a single data symbol is associated with several consecutive pulses, each located in its own frame. Multiple access to the transmission channel is made possible by changing the pulse position within a frame according to a user-specific time-hopping code. Thus, timing recovery may be conveniently viewed as a two-part process

*This research has been funded in part by one or more of the following grants or organizations: ONR N-000140410273, Center for Embedded Networked Systems (NSF STC CCR-01-20778), NSF NRT ANI-0335302, NSF ITR CCF-0313392, NSF Special Projects ANI-0137091, the Okawa Foundation, USC WISE Program, the Intel Foundation, NSF ANI-0087761, NSF CCR-0073505, and by the Italian Ministry of Education in the framework of the project PRIMO, FIRB 2001

[3]. The first part consists of estimating the beginning of the individual frames relative to receiver clock ticks running at frame rate and is called frame timing (FT). The second part consists of identifying the first frame of each symbol in the incoming frame stream and is referred to as symbol timing (ST). The FT problem is approached in [7] by looking for a peak of the correlation between the received waveform and a locally generated template of the transmitted signal. Various search strategies are investigated and compared in terms of mean acquisition time. This is particularly important in the context of UWB communications since UWB signals are characterized by low power spectral density and low overall transmission power. As a consequence, long training sequences are needed to achieve high probability of acquisition. However, a large number of pilot symbols might not be feasible in the presence of a time-varying channel and in general is not desirable since it reduces the spectral efficiency of the system.

Maximum-likelihood techniques (ML) have been investigated in [5]. Both, training-based and blind strategies are proposed and the solution involves sub-pulse sampling. A different approach to ST based on frame-rate samples is proposed in [12]. It operates in a blind fashion and hinges on the cyclo-stationary nature of the UWB signals resulting into a long acquisition time.

In this work, we propose a semi-blind synchronization scheme based on ML techniques to recover ST and FT. Semi-blind schemes combine the methods of channel and timing acquisition based on a pilot signal and blind channel and timing recovery from the information bearing signal [1]. Channel estimation is viewed as a by-product, which can be exploited or not, depending on the detection scheme (coherent or transmitted reference). Simulation results indicate that the semi-blind scheme achieves acquisition rapidly and can successfully be employed in conjunction with both coherent and TR detection. Due to the long multipath delay spread in UWB systems the assumption of independence of the decision statistics proves invalid [4, 13] and the performance of the proposed algorithm is assessed by modeling the decision statistics as correlated Gaussian random variables.

The paper is organized as follows. In Section 2 we present the signal model and introduce the basic notation. Section 3 describes the semi-blind ML timing estimator. The performance of the proposed algorithm is analyzed in Section 4. Simulation results are discussed in Section 5 and conclusions are drawn in Section 6.

2 Signal Model

The transmitted signal is an antipodal modulated signal with time-hopping and is expressed as

$$s(t) = \sum_i a_i \sum_{j=0}^{N_f-1} g(t - iN_fT_f - jT_f - c_jT_c), \tag{1}$$

where $\{a_i\}$ are the information symbols taking values ± 1 with equal probability, $g(t)$ is the elementary pulse (referred to as monocycle), N_f is the number of frames per symbol, T_f is the frame period, T_c is the chip period, and $\{c_i\}_{i=0}^{N_f-1}$ is the time-hopping sequence whose elements are integer values randomly chosen in the range $0 \leq c_i \leq N_h$. We assume that there is no inter-frame interference. This requires that the frame period T_f exceeds the channel delay spread plus the maximum difference between consecutive time shifts of the hopping code.

The received waveform is modeled as

$$r(t) = \sum_i a_i \sum_{j=0}^{N_f-1} \sum_{l=1}^{N_p} \gamma_l g(t - iN_fT_f - jT_f - c_jT_c - \nu T_f - \tau_l) + n'(t). \tag{2}$$

Here, γ_l and τ_l represent the gain and delay associated to the l-th channel path, N_p is the number of paths, $\nu \in [0, N_f - 1]$ is an integer reflecting the hopping-code misalignment between the transmitter and the receiver in a scale of multiples of T_f , and $n'(t)$ is AWGN with two-sided PSD $N_0/2$. Without loss of generality we assume that the minimum path delay $\tau_{\min} = \min_l\{\tau_l\}$ is smaller than the frame duration T_f. Indeed, if it were larger, say a multiple of T_f plus a fraction, then the multiple part could be absorbed into the code misalignment νT_f. The received waveform is passed through a receive filter $g_R(t)$ and is sampled with period $T_s = T_f/Q$, a sub-multiple of T_f. The filter output is

$$r(t) = \sum_i a_i \sum_{j=0}^{N_f-1} \sum_{l=1}^{N_p} \gamma_l g'(t - iN_f T_f - jT_f - c_j T_c - \nu T_f - \tau_l) + n(t), \tag{3}$$

where $g'(t)$ is the convolution $g(t) * g_R(t)$ and $n(t)$ represents the filtered noise. This equation may be rewritten in a more convenient form by denoting μ the integer part of $\tau_{\min}/T_s$ and letting $\varepsilon_l = \tau_l - \mu T_s$ be the fractional delay, where T_s is the sampling period. Note that μ takes values in the range $0 \le \mu \le Q-1$ since $\tau_{\min} < T_f$ by assumption. Substituting ε_l into (3) and rearranging yields

$$r(t) = \sum_i a_i \sum_{j=0}^{N_f-1} h(t - iN_f T_f - jT_f - c_j T_c - \nu T_f - \mu T_s) + n(t), \tag{4}$$

with the channel response (CR) $h(t) \triangleq \sum_{l=1}^{N_p} \gamma_l g'(t - \epsilon_l)$. The signal component corresponding to the symbol a_k is

$$s_k(t) = a_k \sum_{j=0}^{N_f-1} h(t - kN_f T_f - jT_f - c_j T_c - \nu T_f - \mu T_s). \tag{5}$$

Matched-filter detection requires knowledge of $h(t)$, μ and ν. With reference to Figure 1, the parameter ν identifies the first frame of $s_k(t)$ (beginning at $t = kN_f T_f + \nu T_f$) while μ indicates the frames starting times (at $mT_f + \mu T_s$ with $m = 0, 1, 2, \ldots$). Let $\mathbf{h} = [h[0], h[1], \ldots, h[L-1]]^T$ be the sampled version of the CR and denote by $\mathbf{p}(\mu, \mathbf{h})$ the Q-dimensional vector obtained from $\mathbf{h}$ as follows

$$\mathbf{p}(\mu, \mathbf{h}) = [\underbrace{0, 0, \ldots, 0}_{\mu}, h[0], h[1], ..., h[L-1], \underbrace{0, 0, ..., 0}_{Q-L-\mu}]^T. \tag{6}$$

The received signal $r(t)$ in an observation interval of K symbols is sampled with period T_s and its samples are stored in $\mathbf{r}$. In the noise-free case, the received vector corresponding to the kth data symbol can be written as $\mathbf{r}_k = a_k \mathbf{s}_k$, where

$$\mathbf{s}_0 = \left[\left(\mathbf{J}_\mu^1 \mathbf{p}(N_c c_{N_f-1-\nu}, \mathbf{h}) \right)^T, \mathbf{p}(N_c c_{N_f-\nu}, \mathbf{h})^T, \ldots, \mathbf{p}(N_c c_{N_f-1}, \mathbf{h})^T \right]^T \tag{7}$$

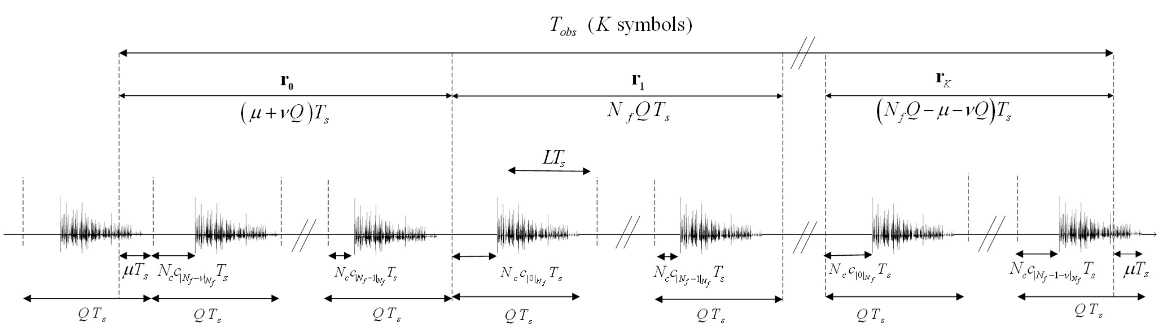

Figure 1: Noise-free component of the received waveform.

$$\mathbf{s}_k = \left[\mathbf{p}(N_c c_0,\mathbf{h})^T, \mathbf{p}(N_c c_1,\mathbf{h})^T, \ldots, \mathbf{p}(N_c c_{N_f-1},\mathbf{h})^T\right]^T, \qquad k \neq 0, k \neq K, \tag{8}$$

$$\mathbf{s}_K = \left[\mathbf{p}(N_c c_0,\mathbf{h})^T, \mathbf{p}(N_c c_1,\mathbf{h})^T, \ldots, \left(\mathbf{J}^2_{Q-\mu-1}\mathbf{p}(N_c c_{N_f-1-\nu},\mathbf{h})\right)^T\right]^T. \tag{9}$$

Here, $\mathbf{J}^1_l = \left[\mathbf{0}_{l\times(N_fQ-l)}\ \mathbf{I}_l\right]$ and $\mathbf{J}^2_l = \left[\mathbf{I}_l\ \mathbf{0}_{l\times N_fQ-l}\right]$ are selection matrices where $\mathbf{I}_l$ is the $l\times l$ identity matrix and $\mathbf{0}_{l\times(N_fQ-l)}$ is an all zero matrix. To focus on the algorithm rather than the notation we disregard $\mathbf{r}_0$ and $\mathbf{r}_K$ (which account for edge effects) and concentrate on $\{\mathbf{r}_k\}_{k=1}^{K-1}$, *i.e.* $K-1$ symbols.

Assuming that the first N_t symbols $[a_1,\ldots,a_{N_t}]$ are known, while the remaining $K-N_t-1$ are not, the likelihood function can be written as

$$\Lambda(\mu,\nu,\mathbf{h}) \propto \exp\left(-\frac{1}{2\sigma^2}\sum_{k=1}^{N_t}\|\mathbf{r}_k - a_k\mathbf{s}_k\|^2\right)\sum_{a_{N_t+1},\ldots,a_{K-1}\in\pm1}\exp\left(-\frac{1}{2\sigma^2}\sum_{k=N_t+1}^{K-1}\|\mathbf{r}_k - a_k\mathbf{s}_k\|^2\right), \tag{10}$$

where the $K-N_t-1$ unknown symbols have been averaged out. With reference to Figure 1, the length-N_fQ received vector $\mathbf{r}_k$, $k=1,2,\ldots K-1$ can be expressed as

$$\mathbf{r}_k = \left[r\left[\mu+\nu Q+(k-1)N_fQ\right],\cdots,r\left[\mu+\nu Q+kN_fQ-1\right]\right]^T. \tag{11}$$

In the next section we discuss a semi-blind maximum likelihood approach for jointly estimating $\mathbf{h}$, ν and μ.

3 Semi-Blind ML Synchronization Algorithm

We denote by $\tilde{\mathbf{s}}_k$ a trial value of $\mathbf{s}_k$ (depending on $\tilde{\mu}$, $\tilde{\nu}$ and $\tilde{\mathbf{h}}$) and $\tilde{\mathbf{r}}_k$ a trial value of $\mathbf{r}_k$ (depending on $\tilde{\mu}$ and $\tilde{\nu}$, as it is seen from (11)). Since the received vector is linear in $\mathbf{h}$, a joint optimization with respect to the parameters $\mathbf{h}$, ν, and μ reduces to a non-linear search with respect to ν and μ. For fixed $\tilde{\mu}$ and $\tilde{\nu}$ and using manipulations similar to [6], the estimate of the CR is obtained as

$$\tilde{h}[l] = \frac{1}{N_f(K-1)}\left(\sum_{k=1}^{N_t}a_k\tilde{r}_{k,l} + \sum_{k=N_t+1}^{K-1}\tanh\left(\frac{\tilde{\mathbf{r}}_k^T\tilde{\mathbf{s}}}{\sigma^2}\right)\tilde{r}_{k,l}\right), \tag{12}$$

where

$$\tilde{\mathbf{r}}_k = \left[r\left[\tilde{\mu}+\tilde{\nu}Q+(k-1)N_fQ\right],\cdots,r\left[\tilde{\mu}+\tilde{\nu}Q+kN_fQ-1\right]\right]^T, \tag{13}$$

$$\tilde{\mathbf{s}} = \left[\mathbf{p}(N_c c_0,\tilde{\mathbf{h}})^T, \mathbf{p}(N_c c_1,\tilde{\mathbf{h}})^T, \ldots, \mathbf{p}(N_c c_{N_f-1},\tilde{\mathbf{h}})^T\right]^T, \tag{14}$$

and

$$\tilde{r}_{k,l} = \sum_{i=\tilde{\nu}+(k-1)N_f}^{\tilde{\nu}+kN_f-1} r\left[l + N_c c_{i-(k-1)N_f-\tilde{\nu}} + \tilde{\mu} + iQ\right]. \tag{15}$$

Thus $\tilde{h}[l]$ can be interpreted as a weighted average of known and estimated data symbols. It is worth noting that (12) is not an explicit expression of $\tilde{h}[l]$ in that $\mathbf{s}_k$ in the right hand side is in its turn a function of $\tilde{h}[l]$. Substituting (12) back in (7) and making the approximation (valid for low SNR) $\log\cosh(x)\approx x^2/2$, the approximate log-likelihood function is obtained as

$$\log\Lambda(\tilde{\mu},\tilde{\nu}) \propto \sum_{k=1}^{N_t}a_k\tilde{\mathbf{r}}_k^T\tilde{\mathbf{s}} + \frac{1}{\sigma^2}\sum_{k=N_t+1}^{K-1}\left(\tilde{\mathbf{r}}_k^T\tilde{\mathbf{s}}\right)^2 - \sum_{k=N_t+1}^{K-1}\tilde{\mathbf{s}}^T\tilde{\mathbf{s}}. \tag{16}$$

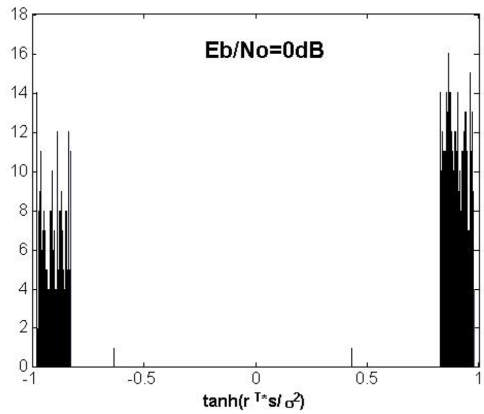

Figure 2: Histogram of the soft-decisions for E_b/N_0=0 dB.

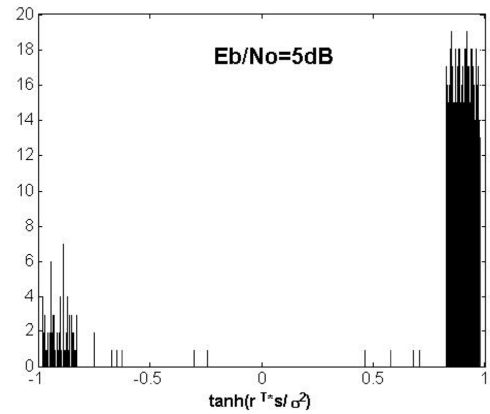

Figure 3: Histogram of the soft-decisions for E_b/N_0=5 dB.

Note that the first term in (16) involves the training symbols, whereas the second and third represent the blind part of the algorithm. Finally, the estimates of μ and ν are computed by maximizing the log-likelihood function in (16), *i.e.*:

$$\{\hat{\mu}, \hat{\nu}\} = \arg\max_{\tilde{\mu},\tilde{\nu}} \{\log \Lambda (\tilde{\mu}, \tilde{\nu})\}, \tag{17}$$

for $\tilde{\mu} = [0, 1, \ldots, Q-1]$ and $\tilde{\nu} = [0, 1, \ldots, N_f - 1]$.

One might be tempted to view the tanh()-terms in (12) as a soft-estimate of the data symbols. However, in our experiments we observed that the argument of the tanh()-terms is large ($\gg 1$) for most of the noise realizations. Figures 2 and 3 show a histogram of the soft-estimates for a SNR of 0 dB and 5 dB when the transmitted data is set to $a_i = +1$. It can be observed that independent of the SNR, the estimates are essentially hard-decisions. What changes with increasing SNR is the probability that the estimated data symbol is correct. Therefore, without noticeable degradation in performance, we can replace tanh() by sign() and obtain an iterative decision-directed algorithm.

The reason for not obtaining soft-decisions is manifold. First, both the received signal vector as well as the template estimate are noisy, causing a large variance at the correlator output. Second, (12) is initialized by an estimate of the CIR based on the pilot-symbols only. Thereafter, estimates of the unknown data symbols are made and a new (hopefully more accurate) template estimate is obtained. Having more than one iteration, on the one hand, reduces the BER on the soft-decisions at each stage of the recursion; on the other hand, it also introduces correlation between the received signal vector and the template estimate. This correlation can be avoided by implementing a computationally more expensive GLRT-like scheme [6].

An iterative structure similar to (12) based on the EM-algorithm is proposed in [11] for a CDMA system. Soft estimates are taken on the 'missing' data (E-step) and based on these decisions the time-varying channel is estimated using a Kalman filter (M-step). In [11], soft-decisions on the unknown data symbols appear to be more reliable due to the reduced dimensionality of the CIR and the problems mentioned above have a reduced impact on the performance of the algorithm. In a realistic UWB scenario however, this is no longer the case as can be observed in Figure 2 and 3.

Finally, observe that the algorithm does not provide any reliability information for the channel estimate during the iterations (*i.e.* noisy template) which appears in the argument of the tanh()-terms. A possible way to deal with this problem would be implementing a turbo-like iterative scheme which performs joint detection and channel estimation. Unfortunately, in order for the turbo algorithm to be effective, prior knowledge on the statistical distribution of the channel impulse response is needed. In the context of

UWB communications this is quite a challenging task since the statistical description of the channel parameters as given in [8] rules out the possibility of deriving an analytically tractable model for the statistics of $\mathbf{h}$.

4 Performance Analysis

In this section, we provide an analysis of the probability of acquisition under the simplifying assumption that the FT is acquired correctly, that is we assume $\tilde{\mu} = \mu$ and we concentrate on the symbol timing. The justification is that small FT errors do not entail significant degradation in the receiver performance. Indeed, for $\hat{\mu} < \mu$, the CR as seen by the receiver is $[0, 0, \ldots, 0, h[0], h[1], \ldots, h[L-1+\hat{\mu}-\mu]]^T$ with $\mu - \hat{\mu}$ zeros at the beginning. Vice versa, for $\tilde{\mu} > \mu$, it is $[h[\hat{\mu}-\mu], \ldots, h[L-1], 0, 0, \ldots, 0]^T$. As long as $|\hat{\mu}-\mu|$ is limited to a few samples the energy of the CR does not change much. In contrast, a ST error deteriorates the BER performance since the phase of the time-hopping code is not estimated correctly. Furthermore, to simplify the analysis we focus on a training-based scheme which uses M pilot symbols to form the template. Notice that this corresponds to setting $N_t = K-1 = M$ in (16), *i.e.* assuming high SNR such that the soft-estimates in (12) are replaced by the actual data symbols.

The output decision statistics

$$D(\tilde{\nu}) = \log \Lambda\left(\mu, \tilde{\nu}\right) \tag{18}$$

for $\tilde{\nu} = 0, \ldots, N_f - 1$, are modeled as correlated Gaussian random variables. An independence assumption usually employed in the analysis of synchronization algorithms [4, 13] is not justified for UWB systems due to the long delay spread of the channel response. Once the first and second moments of $D(\tilde{\nu})$ are known, we employ the union bound to determine the probability of acquisition

$$P_{\text{acq}} = 1 - \Pr\left\{\bigcup_{\tilde{\nu}\neq 0}\{D(\tilde{\nu}) > D(0)\}\right\} \geq 1 - \sum_{\tilde{\nu}\neq 0} \Pr\left\{D\left(\tilde{\nu}\right) - D\left(0\right) > 0\right\}, \tag{19}$$

where $D(0)$ corresponds to the correct hypothesis. A detailed derivation of the results presented in the sequel can be found in [2].

Before we calculate the first and second moments of $\mathrm{D}(\tilde{\nu})$, we rewrite the decision statistics in a form that shows explicitly the dependence on the received signal. Consider the expression of the decision statistic for a training-based scheme with M pilot symbols

$$D\left(\tilde{\nu}\right) = \left(\sum_{k=1}^{M} a_k \tilde{\mathbf{r}}_k^T\right)\tilde{\mathbf{s}}. \tag{20}$$

The received vector $\tilde{\mathbf{r}}_k$ can be partitioned into N_f sub-vectors $\tilde{\mathbf{r}}_{k,m}$ of length Q

$$\tilde{\mathbf{r}}_k = \left[\tilde{\mathbf{r}}_{k,0}^T, \ldots, \tilde{\mathbf{r}}_{k,\tilde{\nu}-1}^T, \tilde{\mathbf{r}}_{k,\tilde{\nu}}^T, \ldots, \tilde{\mathbf{r}}_{k,N_f-1}^T\right]^T, \tag{21}$$

given by $\tilde{\mathbf{r}}_{k,m} = b_{k,m}\tilde{\mathbf{m}}_m + \tilde{\mathbf{n}}_{k,m}$, where $\tilde{\mathbf{m}}_n$ and $\tilde{\mathbf{n}}_{k,n}$ are the mean and the noise of the received vector, $b_{k,m} = a_{k-1}$ for $m \in [0, \tilde{\nu}-1]$ and $b_{k,m} = a_k$ for $m \in [\tilde{\nu}, N_f - 1]$. Defining the matrices

$$\mathbf{T}_m = \left[\begin{array}{ccc} \mathbf{0}_{L\times c_m N_c} & \mathbf{I}_L & \mathbf{0}_{L\times\left(N_f N - L - c_m N_c\right)} \end{array}\right] \tag{22}$$

of dimension $L \times N_f N$ that select only the non-zero elements according to our hypothesis, the channel estimate can be rewritten as

$$\tilde{\mathbf{h}} = \frac{1}{N_f M}\sum_{k=1}^{M}\sum_{n=0}^{N_f-1} a_k \mathbf{T}_n \tilde{\mathbf{r}}_{k,n}. \tag{23}$$

Similarly, the template vector can be partitioned as

$$\tilde{\mathbf{s}} = \left[\tilde{\mathbf{s}}_0^T, \tilde{\mathbf{s}}_1^T \ldots, \tilde{\mathbf{s}}_{N_f-1}^T\right]^T, \tag{24}$$

where the sub-vectors are given by

$$\tilde{\mathbf{s}}_m = \left[\mathbf{0}_{1\times c_m N_c}, \tilde{\mathbf{h}}, \mathbf{0}_{1\times\left(N_f N - L - c_m N_c\right)}\right]^T. \tag{25}$$

Using the results above and neglecting the constant factor $1/((M-1)N_f)$ the decision statistic in (20) can be written as

$$D(\tilde{\nu}) \propto \left\| \sum_{r=1}^{M} \sum_{n=0}^{N_f-1} a_r \mathbf{T}_n \tilde{\mathbf{r}}_{r,n} \right\|^2. \tag{26}$$

With the model provided above, and denoting $\tilde{\mathbf{t}}_n = \mathbf{T}_n \tilde{\mathbf{m}}_n$, it can be easily verified that the first moment and the variance are obtained as

$$\mathrm{E}\left\{D\left(\tilde{\nu}\right)\right\} = M\left(\tilde{\mathbf{t}}_{0,0}^{\tilde{\nu},\tilde{\nu}} + M\tilde{\mathbf{t}}_{\tilde{\nu},\tilde{\nu}}^{N_f,N_f}\right) + MLN_f\sigma^2 \tag{27}$$

$$\begin{aligned}
\sigma^2_{D(\tilde{\nu})} &= \mathrm{E}\left\{D\left(\tilde{\nu}\right)^2\right\} - \mathrm{E}\left\{D\left(\tilde{\nu}\right)\right\}^2 \\
&= \left(2(M-1)^2 - 6(M-1) + 4\right)\left(\tilde{\mathbf{t}}_{0,0}^{\tilde{\nu},\tilde{\nu}}\right)^2 + 4M^3\left(\tilde{\mathbf{t}}_{\tilde{\nu},0}^{N_f,\tilde{\nu}}\right)^2 \\
&+ 4M^2N_f\sigma^2\left(\tilde{\mathbf{t}}_{0,0}^{\tilde{\nu},\tilde{\nu}} + M\tilde{\mathbf{t}}_{\tilde{\nu},\tilde{\nu}}^{N_f,N_f}\right) + 2LM^2N_f^2\sigma^4,
\end{aligned} \tag{28}$$

where

$$\tilde{\mathbf{t}}_{0,0}^{\tilde{\nu},\tilde{\nu}} = \sum_{i=0}^{\tilde{\nu}-1}\sum_{j=0}^{\tilde{\nu}-1} \tilde{\mathbf{t}}_i^T\tilde{\mathbf{t}}_j, \quad \tilde{\mathbf{t}}_{\tilde{\nu},\tilde{\nu}}^{N_f,N_f} = \sum_{i=\tilde{\nu}}^{N_f-1}\sum_{j=\tilde{\nu}}^{N_f-1} \tilde{\mathbf{t}}_i^T\tilde{\mathbf{t}}_j, \quad \tilde{\mathbf{t}}_{\tilde{\nu},0}^{N_f,\tilde{\nu}} = \sum_{i=\tilde{\nu}}^{N_f-1}\sum_{j=0}^{\tilde{\nu}} \tilde{\mathbf{t}}_i^T\tilde{\mathbf{t}}_j. \tag{29}$$

With correct ST (27) and (29) become

$$\begin{aligned}
E\left\{D(0)\right\} &= M^2N_f^2\left\|\mathbf{h}\right\|^2 + MLN_f\sigma^2 \\
\sigma^2_{D(0)} &= 2\sigma^2M^2N_f^2\left(2MN_f\left\|\mathbf{h}\right\|^2 + \sigma^2 L\right).
\end{aligned} \tag{30}$$

The last term to be calculated is the cross-correlation $\mathrm{E}\left\{D(0)D(\tilde{\nu})\right\}$. After some manipulations [2], we obtain

$$\begin{aligned}
\mathrm{E}\left\{D(0)D\left(\tilde{\nu}\right)\right\} &= \left(M^3N_f^2\left\|\mathbf{h}\right\|^2 + M^2N_fL\sigma^2\right)\left(\tilde{\mathbf{t}}_{0,0}^{\tilde{\nu},\tilde{\nu}} + M\tilde{\mathbf{t}}_{\tilde{\nu},\tilde{\nu}}^{N_f,N_f}\right) \\
&+ 4\sigma^2M^2\sum_{i=0}^{N_f-1}\left(\tilde{\nu}\sum_{j=0}^{\tilde{\nu}-1}\tilde{\mathbf{t}}_j^T\tilde{\mathbf{t}}_i + \left(N_f-\tilde{\nu}\right)M\sum_{j=\tilde{\nu}}^{N_f-1}\tilde{\mathbf{t}}_j^T\tilde{\mathbf{t}}_i\right) \\
&+ M^3N_f^3L\sigma^2\left\|\mathbf{h}\right\|^2 + M^2N_f^2L^2\sigma^4 \\
&+ 2\left(M^2\left(N_f-\tilde{\nu}\right)^2 + M\tilde{\nu}^2\right)L\sigma^4.
\end{aligned} \tag{31}$$

Introducing the variable $\tilde{z} = D(\tilde{\nu}) - D(0)$, the probability that the "bin" corresponding to a wrong trial value is larger than the true one can be written as

$$\mathrm{P}(\tilde{z} > 0) = \mathrm{Q}\left(\sqrt{\frac{m_{\tilde{z}}^2}{\sigma_{\tilde{z}}^2}}\right), \tag{32}$$

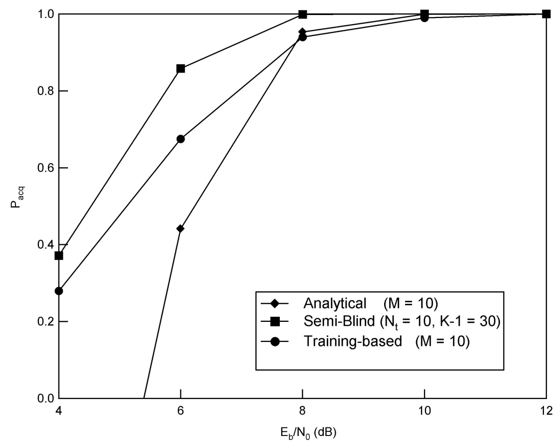

Figure 4: Probability of Acquisition vs E_b/N_0: Analytical and numerical results for semi-blind and training-based scheme ($M = N_t = 10$, $K-1 = 30$).

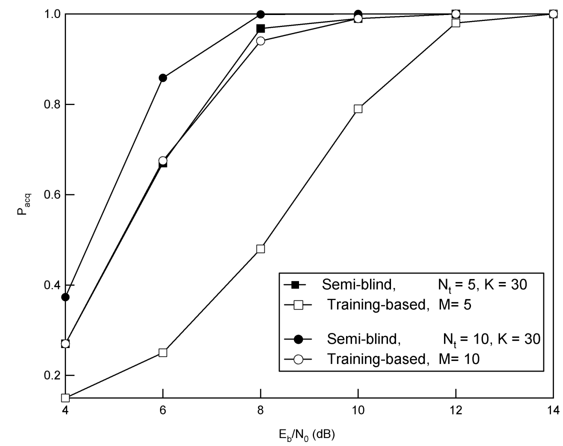

Figure 5: Probability of Acquisition vs E_b/N_0: Comparison between semi-blind and training-based scheme ($M = N_t = 5$, $M = N_t = 10$, $K-1 = 30$).

where $m_{\tilde{z}}$ and $\sigma^2_{\tilde{z}}$ denote the mean and the variance of z, respectively and are given as

$$\begin{aligned} m_{\tilde{z}} &= \mathrm{E}\left\{D(\tilde{\nu}) - D(0)\right\} \\ \sigma^2_{\tilde{z}} &= \sigma^2_{D(\tilde{\nu})} + \sigma^2_{D(0)} - 2\mathrm{E}\left\{D\left(\tilde{\nu}\right) D\left(0\right)\right\} \mathrm{E}\left\{D\left(\tilde{\nu}\right)\right\} \mathrm{E}\left\{D\left(0\right)\right\}. \end{aligned} \tag{33}$$

Substituting into (19) we obtain a lower bound for the probability of acquisition of the training-based synchronization strategy in (20).

5 Simulation Results

We assume a single user scenario. The pulse $g(t)$ is shaped as the second derivative of a Gaussian function and has a width of 1 ns. The frame period T_f is set equal to 110 ns, the number of frames per symbol N_f is 25, the chip period T_c is 2 ns, and the elements of the time-hopping code are randomly chosen in the interval $0 \leq c_j \leq 24$. The receive filter has a rectangular transfer function over $\pm 4GHz$ and the sampling rate Q/T_f is 8 GHz. The Nyquist rate corresponds to $Q = 880$ samples per frame. The performance of the estimation algorithms are expressed as functions of the SNR and the probability of acquisition. The former is defined as the ratio E_b/N_0, where E_b is the energy per symbol at the filter output (before sampling). The channel is modelled as indicated in the report [8] of the IEEE 802.15.3a task group.

5.1 Probability of Acquisition

Our criterion for declaring that the receiver is synchronized is that correct ST is achieved. As mentioned in the previous section, the receiver can cope with an offset of a few samples with respect to the FT without serious degradation of the performance. Therefore, we assume perfect FT, *i.e.* $\hat{\mu} = \mu$. The lower bound on the probability of acquisition derived in Section 4 is shown in Figure 4 for $M = 10$. For moderate to high SNR the analytical expression provided in (19) is in good agreement with the numerical results obtained setting $K-1 = N_t = M = 10$ in (16). As expected, (19) represents a lower bound also for the proposed semi-blind strategy which exploits $N_t = 10$ pilot symbols and $K - 1 - N_t = 20$ unknown data symbols.

In Figure 5, the semi-blind strategy in (16) is compared to a training-based scheme which uses M pilot symbols to form the template. The parameters N_t and M are varied

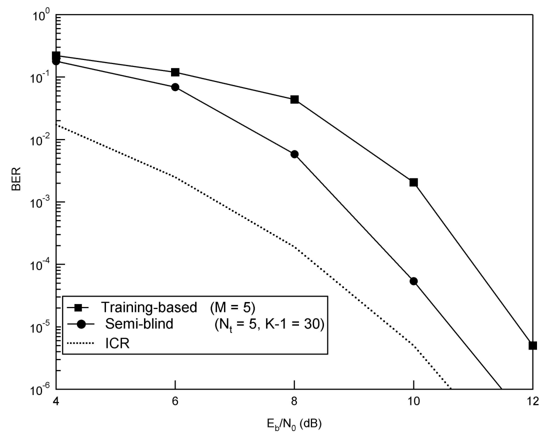

Figure 6: BER vs E_b/N_0 for a correlation receiver: Comparing semi-blind and training-based scheme ($M = N_t = 5$, $K-1 = 30$).

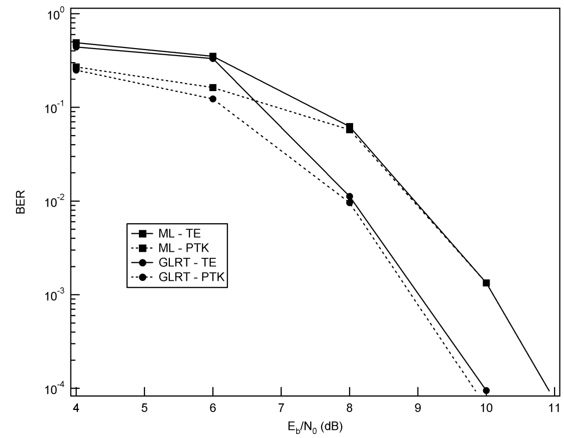

Figure 7: BER vs E_b/N_0 for the GLRT and the ML receiver with ideal and estimated timing parameters ($N_t = 5$ and $K-1 = 30$).

from $M = N_t = 5$ to $M = N_t = 10$ and $K - 1 = 30$. Note that the former exhibits higher probability of acquisition, *i.e.* it requires shorter acquisition time for the same probability of acquisition, which represents a significant advantage when only a few pilot symbols are available at the receiver for synchronization and channel estimation.

5.2 BER performance

In the previous section we evaluated and compared the probability of acquisition of the proposed blind scheme assuming perfect frame alignment. In order to complete the analysis, we now present BER performance results which have been obtained averaging over several channel realizations but selecting only the cases where $\hat{\nu} = \nu$. By doing so we are able to isolate ST from FT and to evaluate the accuracy of both frame level acquisition and channel estimation. In fact, as noted at the beginning of Section 4, an error in the frame timing corresponds to an increase in the number of zero valued taps in the estimated channel response and results into a lower energy capture, which degrades the BER of a receiver provided with such estimates.

The BER performance of the blind strategy in comparison to a training-based scheme which uses $M = 5$ pilot symbols is shown in Figure 6. The correlation receiver is provided with both timing and channel estimates obtained with the two strategies mentioned above. The BER curve of an ideal correlation receiver (ICR) with perfect timing and channel estimates is also shown. It is seen that the blind technique outperforms the other scheme by almost 2 dB and is about 1 dB far away from the ideal case.

Finally the BER results in Figure 7 correspond to a transmitted reference (TR) receiver employing either maximum-likelihood (ML) or generalized likelihood ratio test (GLRT) decision criterion [6]. Two different scenarios are considered. In the first, perfect knowledge of the timing parameters (PTK) is assumed whereas, in the second, both receivers are fed with timing estimates (TE) obtained from (17). Also, we have set $N_t = 5$ and $K - 1 = 30$. The template vector for the ML receiver is obtained from (12) setting $\tilde{\mu} = \hat{\mu}$ and $\tilde{\nu} = \hat{\nu}$, whereas the template vector for the jth data symbol in case of the GLRT receiver is obtained by using

$$\hat{h}_j[l] = \frac{1}{N_f(K-1)} \left(\sum_{k=1}^{N_t} a_k \hat{r}_{k,l} + \sum_{k=N_t+1, k\neq j}^{K-1} \tanh\left(\frac{\hat{\mathbf{r}}_k^T \hat{\mathbf{s}}_k}{\sigma^2} \right) \hat{r}_{k,l} \right), \tag{34}$$

where $\hat{\mathbf{r}}_k$, $\hat{\mathbf{s}}_k$ and $\hat{r}_{k,l}$ are given by (13)-(15) replacing ($\tilde{\mu}$, $\tilde{\nu}$) with the estimated timing parameters ($\hat{\mu}$, $\hat{\nu}$). Note that (34) requires the calculation of a different vector $\hat{\mathbf{h}}_j =$

$[\hat{h}_j[1], \hat{h}_j[2], \ldots, \hat{h}_j[L-1]]^T$ for each data symbol a_j. Thus the GLRT receiver is more complex than the ML-based receiver.

It is seen that for moderate to high SNR the GLRT outperforms the ML receiver by approximately 1 dB. This fact is explained observing that the correlation between the template and the incoming waveform generates a non-Gaussian cross noise term which degrades the BER. This term is not present when the GLRT rule is applied (the sum over k in (34) does not include the index j). Furthermore, both receivers converge to their ideal counterparts at moderately low SNR.

6 Conclusions

We have described a semi-blind ML-based channel and timing estimation algorithm that recovers both symbol and frame timing. Channel estimation is inherent in the timing acquisition algorithm and can be used for data detection. The proposed scheme uses N_t pilot symbols to initialize the recursive computation of the CR and then operates blindly over the remaining observed symbols taking 'soft' decisions on the data. In this specific context, we have found that soft-estimates are almost identical to hard-decisions. An explanation of this fact is provided and a lower bound on the probability of acquisition has been derived based on correlated Gaussian random variables.

Simulations show that the semi-blind technique presented here compares favorably with a training-based scheme which uses $M = N_t$ pilot symbols to form the template. Also, the BER of a TR receiver endowed with the estimated parameters and employing a ML and a GLRT detection test has been computed in a realistic scenario.

References

[1] E. Aktas and U. Mitra. Semi-blind channel estimation for CDMA systems with parallel data and pilot signal. *IEEE Trans. Comm.*, 52(7):1102–1112, Jul. 2004.

[2] C. Carbonelli and S. Franz. Semi-blind ML synchronization for TR-UWB systems: performance analysis. May 2004. http://www.ing.unipi.it/~o623499/page4.html.

[3] C. Carbonelli and U. Mengali. Timing recovery for UWB signals. *Proc. IEEE Globecom*, Dec. 2004. Dallas, US.

[4] G. E. Corazza. On the MAX/TC criterion for code acquisition and its application to DS-SSMA systems. *IEEE Trans. Comm.*, 44(9):1173–1182, Sep. 1996.

[5] A. N. D'Andrea, V. Lottici, and U. Mengali. Channel estimation for ultra-wideband communications. *IEEE JSAC*, 3:1638–1645, Dec. 2002.

[6] S. Franz and U. Mitra. On optimal data detection for UWB transmitted reference systems. *Proc. IEEE Globecom*, 2:744–748, Dec. 2003. San Francisco, US.

[7] E. A. Homier and R. A. Scholtz. Rapid acquisition of ultra-wideband signals in the dense multipath channel. *Proc. IEEE UWBST*, pages 245–250, May 2002. Baltimore, US.

[8] http://grouper.ieee.org/groups/802/15/. Channel modeling sub-commitee report final. IEEE P802.15-02/368r5-SG3a, Nov. 2002.

[9] W. M. Lovelace and J. K. Townsend. The effects of timming jitter on the performance of impulse radio. *IEEE JSAC*, 20(9):1646 – 1651, Dec. 2002.

[10] M. Z. Win and R. A. Scholtz. Impulse radio: How it works. *IEEE Communication letters*, 2(2):36–38, Feb. 1998.

[11] M. Yan and B. D. Rao. Soft decision-directed MAP estimate of fast rayleigh flat fading channels. *IEEE Trans. Comm.*, 51(12):1965–1969, Dec 2003.

[12] L. Yang, Z. Tian, and G. B. Giannakis. Non-data aided timing acquisition of ultra-wideband transmissions using cyclostationarity. *Proc. ICASSP*, 4:121–124, Apr. 2003. Hong Kong, China.

[13] M. Yao, F. Chin, B. Kannan, and S. Pasupathy. Acquisition performance of an ultra wide-band communications system over a multiple-access fading channel. *Proc. IEEE UWBST*, pages 99–103, May 2002. Baltimore, US.